Radiative Depopulation of the Excited Intramolecular Charge-Transfer State of 9-(4-(*N*,*N*-Dimethylamino)phenyl)phenanthrene

A. Onkelinx,[†] F. C. De Schryver,*[,†] L. Viaene,[†] M. Van der Auweraer,[†] K. Iwai,[‡] M. Yamamoto,[‡] M. Ichikawa,[§] H. Masuhara,[§] M. Maus,[||] and W. Rettig[||]

Contribution from the Department of Chemistry, Katholieke Universiteit Leuven, Celestijnenlaan 200F, B-3001 Heverlee-Leuven, Belgium, Department of Chemistry, Faculty of Science, Nara Women's University, Nara 630, Japan, Department of Applied Physics, Faculty of Engineering, Osaka University, Suita, Osaka 565, Japan, and Institut für Physikalische und Theoretische Chemie, Humboldt-Universität, Bunsenstrasse 1, D-10117 Berlin, Germany

Received November 2, 1995[⊗]

Abstract: Intramolecular photoinduced electron transfer in 9-(*p*-*N*,*N*-dimethylanilino)phenanthrene (9DPhen) has been studied in solution. The solvent dependence of the fluorescence spectra of 9DPhen indicates that the emission occurs from a highly polar excited state. The quantum yield of fluorescence (Φ_f) of 9DPhen is quite high and increases with increasing solvent polarity. The radiative rate constant (k_f), however, shows a maximum for solvents of intermediate polarity, e.g., in butyl acetate a value of 2.3×10^8 s^{-1} is attained. These results are difficult to explain within the "TICT" (twisted intramolecular charge transfer) model, which predicts a strongly forbidden fluorescence caused by a minimum overlap of the orbitals involved in the transition. The above-mentioned trend as a function of the solvent polarity is observed in particular donor−acceptor substituted arenes where the L_b state of the corresponding arenes is lower in energy than the L_a state. The quantum chemical calculations actually could explain this behavior on the basis of an ICT state which interacts with the lower lying ^1L_a and ^1L_b states of the acceptor. The quantum mechanical mixing of states can occur by two pathways, namely orbital mixing and mixing of configurations, and is modified by geometrical changes and by solvent polarity. The single exponential fluorescence decay, obtained with time-correlated single-photon-timing, suggests emission from an excited charge-transfer state, resulting from a solvent-induced rapid relaxation of the initial delocalized excited state of 9DPhen, obtained immediately after picosecond pulsed excitation. Picosecond transient absorption spectra in acetonitrile show a rapid decay within a few picoseconds from a less polar but delocalized excited state toward a more polar ICT state. Even the triplet state of 9DPhen in isopentane at 77 K shows a significant polar character. As a reference compound, 9-phenylphenanthrene (9PhPhen) was also examined by means of stationary and time-resolved fluorescence measurements as well as transient absorption experiments.

Introduction

For molecules consisting of an electron donor and an electron acceptor moiety coupled by a polymethylene chain,[1−15] excitation is often followed by a conformational folding bringing the donor and the acceptor π-electron systems into parallel planes within a distance allowing through-space interactions and Coulomb stabilization of the charge-transfer (CT) state.[16−18] If the driving force between the donor (D) and acceptor (A) is appropriate, photoinduced electron transfer can occur even in the stretched conformation.[19−23]

[†] Katholieke Universiteit Leuven.
[‡] Nara Women's University.
[§] Osaka University.
[||] Humboldt-Universität.
* To whom correspondence should be addressed.
[⊗] Abstract published in *Advance ACS Abstracts,* March 1, 1996.

(1) Mataga, M.; Okada, T.; Masuhara, H.; Nakashima, N.; Sakata, Y.; Misumi, S. *J. Lumin*. **1976**, *12/13*, 159.
(2) Okada,T.; Saito, T.; Mataga, N.; Sakata, Y.; Misumi, S. *Bull. Chem. Soc. Jpn*. **1977**, *50*, 331.
(3) Migita, M.; Okada, T.; Mataga, N.; Sakata, Y.; Misumi, S.; Nakashima, N.; Yoshihara, K. *Bull. Chem. Soc. Jpn.* **1981**, *54*, 3304.
(4) Okada, T.; Migata, M.; Mataga, N.; Sakata, Y.; Misumi, S. *J. Am. Chem. Soc*. **1981**, *103*, 4715.
(5) Masaki, S.; Okada, T.; Mataga, N.; Sakata, Y.; Misumi, S. *Bull. Chem. Soc. Jpn*. **1976**, *49*, 1277.
(6) Swinnen, A. M.; Van der Auweraer, M.; De Schryver, F. C.; Windels, C.; Goedeweeck, R.; Vannerem, A.; Meeus, F. *Chem. Phys. Lett*. **1983**, *95*, 467.
(7) Swinnen, A. M.; Van der Auweraer, M.; De Schryver, F. C.; *Chem. Phys. Lett*. **1984**, *109*, 574.
(8) Swinnen, A. M.; Van der Auweraer, M.; De Schryver, F. C. *J. Photochem*. **1985**, *28*, 315.
(9) Swinnen, A. M.; Ruttens, F.; Van der Auweraer, M.; De Schryver, F. C. *Chem. Phys. Lett*. **1985**, *116*, 217.
(10) Swinnen, A. M.; Van der Auweraer, M.; De Schryver, F. C.; Nakatani, K.; Okada, T.; Mataga, N. *J. Am. Chem. Soc*. **1987**, *109*, 321.
(11) Hatano, Y.; Yamamoto, M.; Nishijama, Y. *J. Phys. Chem*. **1987**, *82*, 367.
(12) Helsen, N.; Viaene, L.; Van der Auweraer, M.; De Schryver, F. C. *J. Phys. Chem*. **1994**, *98*, 1532.
(13) Okada, T.; Fujita, T.; Kubota, M.; Masaki, S.; Mataga, N.; Hayashi, T.; Ide, R.; Sakata, Y.; Misumi, S. *Chem. Phys. Lett* **1972**, *14*, 563.
(14) De Schryver, F. C.; Van der Auweraer, M.; Boens, N.; Declercq, D.; Helsen, N.; DePaemelaere, S.; Van Haver, P.; Onkelinx, A.; Iwai; K. *Supramol. Chem.* **1992**, 313.
(15) De Schryver; F. C.; Declercq, D.; Depaemelaere, S.; Hermans, E.; Onkelinx, A.; Verhoeven, J. W.; Gelan, J. *J. Photochem. Photobiol. A: Chem*. **1994**, *82*, 171.
(16) Hirayama, F. *J. Chem. Phys.* **1965**, *42*, 3163.
(17) Mimura, T.; Itoh, M. *J. Am. Chem. Soc*. **1976**, *98*, 1095.
(18) Davidson, R. S. In: *Advances in Physical Organic Chemistry*; J. Wiley: New York, 1983; Vol. 19, p 1.
(19) Wegewijs, B.; Hermant, R. M.; Verhoeven, J. W.; Kunst, A. G. M.; Rettschnick, R. P. H. *Chem. Phys. Lett.* **1987**, *140*, 587.
(20) Van Stokkum, I. H. L.; Brouwer, A. M.; Van Ramesdonk, H. J.; Scherer, T. Proc. K. Ned. Akad. Wet. **1993**, *96*, 43.
(21) Verhoeven, J. W. *Pure Appl. Chem*. **1990**, *62*, 1985.
(22) Hermant, R. M.; Wegewijs, B.; Verhoeven, J. W.; Kunst, A. G. M.; Rettscnick, R. P. H. *Recl. Trav. Chim. Pays-Bas* **1988**, *107*, 349.
(23) Wegewijs, B.; Verhoeven, J. W. *J. R. Neth. Chem. Soc.* **1995**, *114*, 1.

0002-7863/96/1518-2892$12.00/0

In another type of molecules with the donor and the acceptor groups directly connected by a single σ-bond, conformational folding is excluded.[24−29] It has been shown[30−53] that primary excited singlet states of *p*-(9-anthryl)-*N*,*N*-dimethylaniline (ADMA) and related compounds undergo solvent-assisted femto/picosecond relaxation to a polar fluorescent CT state. The geometry and electronic structure of the emitting CT state, however, are still a point of discussion.[28,29,34,46] Okada and coworkers[30−32] first explained their results in terms of the TICT (twisted intramolecular charge transfer) state model.[34,54] According to this interpretation, the excited singlet state undergoes an adiabatic intramolecular electron transfer. Two metastable states are assumed to interconvert by a torsional motion, which provides a possible reaction coordinate for the electron transfer. More recent picosecond transient absorption studies however show a difference between the electronic structure of the excited state of ADMA or structurally similar molecules and that of molecules with strongly orthogonal π systems of donor and acceptor (e.g., 4-(9-anthryl)-*N*,*N*,2,6-tetramethylaniline) (ATMA)).[46,49,55] The transient absorption spectra of ADMA in medium polar solvents cannot be represented by a linear combination of the anthracene-like band in weakly polar, and the anthracene anion radical band in strongly polar, solvents,

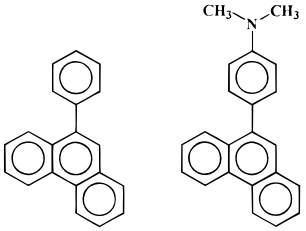

Figure 1. Structures of 9PhPhen and 9Dphen.

so doubts have been expressed as to the validity of the simple two-state TICT model for ADMA and related compounds. Thereby an aryl−amine torsion angle of less than 90° is proposed for the excited states of these compounds.

A similar conclusion was also reached in recent quantum chemical calculations[56] where twist angle dependent values of transition energies, oscillator strengths, and dipole moments were calculated.

Similar to the behavior of ADMA and related compounds, other large conjugated π-systems connected formally by a single bond[29,56−58] indicate a nonorthogonal geometry of the CT state or a TICT state strongly vibronically coupled with a nearby nonpolar state.[59]

A different model, not involving intramolecular twisting, has recently been proposed to explain the dual fluorescence in aminobenzonitriles, the compounds originally explained within the TICT framework.[34,54] In this model the dual emission is interpreted as a solvent-induced pseudo-Jahn−Teller effect: dual fluorescence and intramolecular charge transfer (ICT) are observed when two excited levels S_1 and S_2 (CT) in *N*,*N*-dimethyl-4-aminobenzonitrile (DMABN) have an energy gap sufficiently small for vibronic coupling. It is argued that the N-inversion of the amino group acts as a promoting mode which decouples, even without rotational isomerization, the nitrogen lone pair from the π-electrons of the phenyl ring.[60,61]

This interpretation was based on the observation of intramolecular charge transfer in a series of 4-(dialkylamino)benzonitriles (methyl, ethyl, propyl, and decyl), even in apolar solvents. The observation that the charge separation increased with increasing length of the alkyl chain was difficult to explain within the the former TICT model.

Recently, however, CASSCF (complete active space self-consistent field) calculations[62] seem not to support such an alternative interpretation as the only contributive mechanism to the CT state.

Also in another recent publication[63] where solvent effects have been analyzed using a microstructural solvation model associated with the AM1 results of some parasubstituted *N*,*N*-dimethylaniline derivatives, the same conclusion is obtained. The dual fluorescence phenomena could be related to the presence of a twisted internal charge-transfer state which is stabilized even in a nonpolar solvent but cannot be related only to the presence of a wagged internal charge-transfer state, even in a strongly polar solvent.

(24) Rettig, W. *Angew. Chem., Int. Ed. Engl.* **1986**, *25*, 971.
(25) Hagopian, S.; Singer, L. A. *J. Am. Chem. Soc.* **1985**, *107*, 1874.
(26) Detzer, N.; Baumann, W.; Schwager; B.; Frohling, J.-C.; Brittinger, C. *Z. Naturforsch.* **1987**, *A42*, 395.
(27) Siemiarczuk, A.; Koput, J.; Pohorillo, A. *Z. Naturforsch.* **1982**, *A37*, 598.
(28) Herbich, J.; Kapturkiewicz, A. *Chem. Phys.* **1991**, *158*, 143, and references therein.
(29) Herbich, J.; Kapturkiewicz, A. *Chem. Phys.* **1993**, *170*, 221.
(30) Okada, T.; Fujita, T.; Kubota,M.; Masaki, S.; Mataga,N.; Ide, R.; Sakata, Y.; Misumi, S. *Chem. Phys. Lett.* **1972**, *14*, 563.
(31) Okada, T.; Fujita, T; Mataga, *N. Z. Phys. Chem. NF* **1976**, *101*, 57.
(32) Masaki, S.; Okada, T.; Mataga, N.; Sakata, Y.; Misumi, S. *Bull. Chem. Soc. Jpn.* **1976**, *49*, 1277.
(33) Chandross, E. A. In *The Exciplex*; Gordon, M.; Ware, W.R., Eds.; Academic Press: New York, 1975; p 187.
(34) Grabowski, Z. R.; Rotkiewicz, K.; Siemiarczuk, A.; Cowley, D. J; Baumann, W. *Nouv. J. Chim.* **1979**, *3*, 443.
(35) Grabowski, Z. R.; Dobkowski, J. *Pure Appl. Chem.* ,**1983**, *55*, 245.
(36) Grabowski, Z. R. *Acta Phys. Pol.* **1987**, *A71*, 743.
(37) Grabowski, Z. R. In *Supramolecular Photochemistry*; Balzani, V., Ed.; Reidel: Dordrecht, The Netherlands, 1987; p 319.
(38) Siemiarczuk, A.; Grabowski, Z. R.; Krówczynski, A.; Asher, M.; Ottolenghi, M. *Chem. Phys. Lett.* **1977**, *51*, 315.
(39) Grabowski, Z. R.; Rotkiewicz, K.; Siemiarczuk, A. *J. Lumin.* **1979**, *18/19*, 420.
(40) Siemiarczuk, A. *Chem. Phys. Lett.* **1984**, *110*, 437.
(41) Siemiarczuk, A.; Ware,W. R. *J. Phys. Chem.* **1987**, *91*, 3677.
(42) Baumann, W.; Petzke, F.; Loosen, K. D. *Z. Naturforsch.* **1979**, *A34*, 1070.
(43) Baumann, W.; Bischof, *H. J. Mol. Struct.* **1982**, *84*, 181.
(44) Detzer, N.; Baumann, W.; Scwager, B.; Fröhling, J. C.; Brittinger, C. *Z. Naturforsch.* **1987**, *A42*, 395.
(45) Okada,T.; Kawai, M.; Ikemachi,T.; Mataga, N; Sakata,Y.; Misumi, S.; Shionoya, S. *J. Phys. Chem.* **1984**, *88*, 1976.
(46) Okada,T.; Mataga, N.; Baumann, W.; Siemiarczuk, A. *J. Phys. Chem.* **1987**, *91*, 4490.
(47) Baumann, W.; Schwager, B.; Detzer, N.; Okada, T.; Mataga, N. *J. Phys. Chem.* **1988**, *92*, 3742.
(48) Mataga, N.; Yao, H.; Okada, T.; Rettig, W. *J. Phys. Chem.* **1989**, *93*, 3383.
(49) Mataga, N.; Nishikawa, S.; Asahi, T.; Okada,T. *J. Phys. Chem.* **1990**, *94*, 1443.
(50) Barbara, P. F.; Jarzeba, W. In *Advances in Photochemistry*; Volman, D. H., Hammond, G. S., Gollnick, C., Eds.; Wiley: New York, 1990; Vol. 15, p 1.
(51) Tseng, J. C. C.; Huang, S.; Singer, L. A. *Chem. Phys. Lett.* **1988**, *153*, 401.
(52) Tseng, J. C. C.; Singer, L. A. *J. Phys. Chem.* **1989**, *93*, 7092.
(53) Rettig, W; Baumann, W. In: *Photochemistry and Photophysics*; Rabek, J. F., Ed.; CRC Press: Boca Raton, FL, 1992; Vol. 6, p 79.
(54) Rettig, W. Electron transfer I. In Topics in Current Chemistry, Vol. 169; Mattay, J., Ed.; Spinger Verlag: Berlin, 1994; p 253.
(55) Okada, T. *Proc.−Indian Acad. Sci., Chem. Sci.* **1992**, *104*, 173.
(56) Klock, A. M.; Rettig, W. *Polish. J. Chem.* **1993**, *67*, 1375.
(57) Van Damme, M.; Hofkens, J.; De Schryver, F. C.; Ryan, T. G.; Rettig, W.; Klock, A. M. *Tetrahedron* **1989**, *45*, 4693.
(58) Herbich, J.; Waluk, J. *Chem. Phys* **1994**, *188*, 247.
(59) Dobkowski, J.; Grabowski, Z.; Paeplow, B.; Rettig, W.; Koch, K.; Müllen, K.; Lapouyade, R. *New. J. Chem.* **1994**, *18*, 525.
(60) Schuddeboom, W.; Jonker, S. A.; Warman, J. M.; Leinhos, U.; Kühnle, W.; Zachariasse, K. *J. Phys. Chem.* **1992**, *96*, 10809.
(61) Zachariasse, K.; Von Der Haar; T.; Hebecker, A.; Leinhos, U.; Kühnle, W. *Pure Appl. Chem.* **1993**, *65*, 1745.
(62) Serrano-AndrÇs, L.; Merchan, M.; Roos, B. O.; Lindh, R. *J. Am. Chem. Soc.* **1995**, *117*, 3189.
(63) Gorse, A. D.; Pesquer, M. *J. Phys. Chem.* **1995**, *99*, 4039.

The present contribution concerns the photoinduced electron transfer in phenanthryl−aniline systems. These compounds have some important advantages compared to other aryl systems, e.g. a low tendency to form intermolecular aggregates, the absence of excimer formation,[64] and a high quantum yield of fluorescence.

In this paper we focus on the solvent dependence of the spectral position of the CT fluorescence maxima ($\tilde{\nu}_{max}$), the quantum yield (Φ_f), the excited state depopulation kinetics ($\langle\tau_f\rangle$) and resulting radiative rate constant ($\langle k_f\rangle$).

In order to get more information about the nature of the fluorescent excited states, single photon timing experiments are combined with picosecond transient absorption experiments in a polar and an apolar solvent. To obtain more information about the nature of the triplet state and, more importantly, about the different triplet states in 9DPhen and 9PhPhen, nanosecond transient absorption measurements are executed in combination with phosphorescence experiments in a rigid glass.

Because of the size of the 9DPhen compound, it was practically impossible to perform CASSCF calculations in combination with multiconfigurational second-order perturbation theory (CASPT2) to calculate transition energies (absorption and emission) and structural and electronical properties of the ground and excited states and to compare these findings with available experimental information.

Instead, the semiempirical CNDO/S method of Del Bene and Jaffe modified to cope with larger molecules and to calculate excited-state dipole moments was used with two different parametrizations[65] to calculate transition energies, oscillator strengths, and dipole moments.

Experimental Section

Synthesis. 9-(4-(*N*,*N*-Dimethylamino)phenyl)phenanthrene was synthesized by the Grignard coupling reaction[66] of (4-(*N*,*N*-dimethylamino)-phenyl)magnesium bromide with 9-bromophenanthrene using dichloro-[1,3-bis(diphenylphosphino)propane]nickel(II) catalyst in dry THF. The crude product was purified by column chromatography on silica gel with benzene eluent and recrystallized from hexane: mp 155.5−156.5 °C. EIMS (20 eV): *m/e* (relative intensity) 297 (M^+, 100) and 282 (4). ^{1}H NMR ($CDCl_3$): δ 3.03 (6H, s), 6.71−8.84 (13H, m). 9PhPhen was similarly synthesized from 9-phenanthrylmagnesium bromide and phenyl bromide.

The crude product was purified by column chromatochraphy on silica gel with benzene eluent and recrystallized three times from methanol to yield a white powder: mp 103.5−104.5 °C [lit.[67] 104−104.5 °C].

All solutions used for stationary and time-resolved fluorescence measurements were further purified on HPLC with 10:90 V% ethyl acetate, with hexane as the eluent.

Solvents. The solvents used (isooctane, Merck; *cis*-decaline, Aldrich; dibutyl ether, Merck; diethyl ether, Lab scan; butyl acetate, Janssen Chimica; ethyl acetate, Merck; tetrahydrofuran, Rathburn; butanol, Merck; acetonitrile, Merck) were of spectroscopic grade and were used as received. The solvent diisopropyl ether (Riedel De Haën) was checked for fluorescence before use.

Methods. The absorbance of the sample solutions used for stationary and time-resolved fluorescence measurements equals 0.1 at the excitation wavelength for the fluorescence experiments ($\lambda_{excitation}$ = 295 nm) and 1.5 for the nanosecond transient absorption measurements ($\lambda_{excitation}$ = 320 nm).

Absorption spectra were recorded on a Perkin Elmer Lambda 6 UV/vis spectrophotometer. Corrected fluorescence spectra were obtained with a SPEX Fluorolog 212. The fluorescence quantum yields were determined using quinine sulfate in 0.1 N H_2SO_4(Φ_f = 0.54) as a reference.[68]

Stationary and time-resolved fluorescence measurements were performed on samples degassed by several freeze−pump−thaw cycles.

The picosecond laser photolysis system[69−70] as well as the nanosecond laser photolysis system[71] has been described in detail elsewhere.

Time-resolved fluorescence decays were obtained by the single-photon-timing (SPT) technique, and the fluorescence decays were analyzed by the global analysis as described, using the reference convolution method.[72−75] For the SPT experiments an excitation wavelength of 295 nm (fwmh = 40 ps) was used and decays were measured over the whole emission range (isooctane, 370−470 nm; dibutyl ether, 380−460 nm; diisopropyl ether, 380−460 nm; diethyl ether, 380−460 nm; butyl acetate, 380−460 nm; ethyl acetate, 390−540 nm; tetrahydrofuran, 390−500 nm; ethanol, 440−480 nm; acetonitrile, 380−530 nm). All fluorescence decay curves were observed at the magic angle (55°), contained 10^4 peak counts, and were collected in 511 channels of the multichannel analyzer. Time increments of 60, 62, and 81 ps/channel were used for 9DPhen and 327 ps/channel for 9PhPhen, respectively.

For 9DPhen in acetonitrile the previous experiments were completed with measurements using a time increment of 5 ps as well as a scatter solution (LUDOX) instead of a reference.

POPOP [*p*-bis[2-(5-phenyloxazoyl)]benzene in methylcyclohexane], PPO (2,5-diphenyloxazole) in methylcyclohexane], and MSQ (methoxysulfopropylquinolinium in water), having a decay time (τ) of respectively 1.1, 1.4, and 27 ns at room temperature, were used as reference compounds. The reference samples were degassed by several freeze−pump−thaw cycles before use.

The molecular conformation of 9DPhen has been investigated by X-ray diffraction, and the dihedral angle between the two aromatic ring systems in crystalline 9DPhen was found to be 64.2°.[76]

For the quantum chemical calculations, configuration interaction with 50 singly excited configurations was included. The latter were generated from the usual canonical molecular orbitals which are virtually localized on the submoieties for 90° twist but can extend over the whole π-system for other twist angles (see below Figure 12). The input geometries have been optimized with the AM1 Hamiltonian within the AMPAC program.[77] For comparison, idealized input geometries were also used (regular fully planar hexagons for the phenyl and phenanthrene groups with 1.4 Å *R*(CC), 1.08 Å *R*(CH), and *R*(CC) = 1.50 Å between these two groups and *R*(CN) = 1.37 Å and R(N-CH3) = 1.46 Å for the dimethylamino group). The solvation energies of the excited states were calculated from their dipole moments μ

(64) Chandross, E. A.; Langworth, J. W.; Visco, R. E. *J. Am. Chem. Soc.* **1965**, *87*, 3259.
(65) CNDO/S: Del Bene, J.; Jaffé, H. H. *J. Chem. Phys*. **1968**, *48*, 1807; **1968**, *49*, 1221; **1969**, *50*, 1126. CNDUV: QCPE program no. 333 with the original paramaters was used.
(66) Kumada, M. *Pure Appl. Chem.* **1980**, *52*, 669 and references therein.
(67) Koussini, R.; Lapouyade, R.; de Violet, P. F. *J. Am. Chem. Soc.* **1978**, *100*, 6679.
(68) Morris, J. V.; Mahaney, M. A.; Huber, J. R. *J. Phys. Chem.* **1976**, *80*, 969.
(69) Ichikawa, M.; Fukumura, H.; Masuhara, H. *J. Phys. Chem*. **1994**, *98*, 12211. Ichikawa, M.; Fukumura, H.; Masuhara, H.; Koide, E.; Hyakutake, H. *Chem. Phys. Lett*. **1995**, *232*, 346.
(70) Fukazawa, N.; Fukumura, H.; Masuhara, H.; Prochorow, J. *Chem. Phys. Lett*. **1994**, *220*, 461.
(71) Viaene, L.; Van Mingroot, H.; Van haver, P.; Van der Auweraer, M.; De Schryver, F. C.; Itaya, A.; Masuhara, H. *J. Photochem. Photobiol. A: Chem*. **1992**, *66*, 1.
(72) Khalil, M. M. H.; Boens, N.; Van der Auweraer, M.; Ameloot, M.; Andriessen, R.; Hofkens, J.; De Schryver, F. C. *J. Phys. Chem*. **1991**, *95*, 9375.
(73) O'Connor, D. V.; Phillips, D. *Time-Correlated Single Photon Counting*; Academic Press: London, 1984.
(74) Boens, N.; Janssens, L. D.; De Schryver, F. C. *Biophys. Chem*. **1989**, *33*, 77.
(75) Boens, N. *Luminiscence Techniques in Chemical and Biochemical Analysis*; De Keukeleire, W. R. G., Korkidis, K., Eds.; Marcel Dekker: New York, 1991; pp 21−45.
(76) Van Meervelt, L *Acta Crystallogr*. **1993**, *C49*, 593.
(77) AMPAC 5.0, Semichem, 7128 Summit, Shawnee, KS 66216, 1994.
(78) Onsager, L. *J. Am. Chem. Soc*. **1936**, *58*, 1486.
(79) Jaffé, H.; Orchin, M. *Theory and applications of ultraviolet spectroscopy*; John Wiley and Sons: New York, 1966; p 81.
(80) Onsager, L. *J. Am. Chem. Soc*. **1936**, *58*, 1486.
(81) Lippert, E. *Z. Naturforsch*. **1955**, *10A*, 541.
(82) Mataga, N.; Kaifu, Y.; Koizumi, M. *Bull. Chem. Soc. Jpn*. **1955**, *28*, 690.
(83) McRae, E. G. *J. Phys. Chem*. **1957**, *61*, 562.

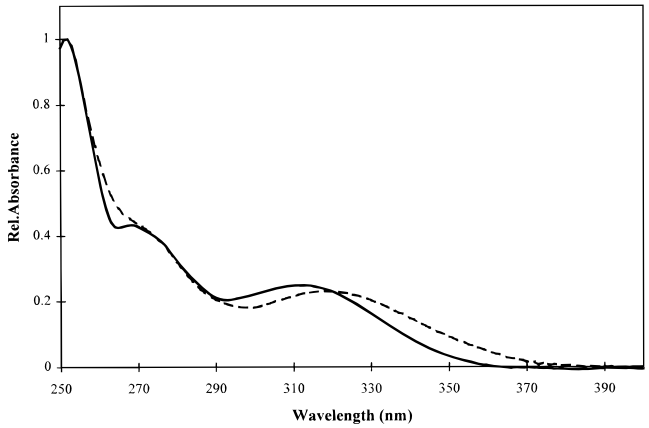

Figure 2. Absorption spectra of 9DPhen in isooctane (—) and acetonitrile (- - -).

(calculated in the gas phase) and the Onsager cavity radius taken as 0.56 nm for 9DPhen using the following equations:[78]

$$E_{solv}(S_n) = E_{gas}(S_0) + \Delta E_{gas}(S_0 \rightarrow S_n) + \Delta E_{solv}(S_n) \quad (1)$$

$$\Delta E_{solv}(S_n) = -\frac{1}{4\pi\epsilon_0}\frac{\mu^2(S_n)}{a^3}\frac{\epsilon_r - 1}{2\epsilon_r + 1} \quad (2)$$

where ϵ_r is the static dielectric constant of the solvent. These calculations were executed on a HP 715 workstation.

Results and Discussion

Absorption and Emission Experiments as a Function of the Solvent Polarity. The absorption spectra of 9DPhen in isooctane and acetonitrile, presented in Figure 2, consist of two absorption bands. The long-wavelength absorption band at 312 nm exhibits a slight bathochromic shift of 700 cm^{-1} upon increasing the solvent polarity from isooctane to acetonitrile. The ^1L_b transition of phenanthrene (^1L_b: 348 nm) is not observed because of its symmetry-forbidden nature and the more intense absorption band around 312 nm. This observation suggests that there is already an interaction between the dimethylanilino and the phenanthryl components in the ground state. The molar extinction coefficient of 9DPhen in isooctane has a value of 15 200 L mol^{-1} cm^{-1} in the maximum of the absorption band (312 nm) and 11 500 L mol^{-1} cm^{-1} in the maximum of the absorption band in acetonitrile, respectively (319 nm).

9DPhen shows a fluorescence emission, which is highly solvatochromic at room temperature as can be seen in Figure 3. The emission spectra lose structure, broaden, and shift to the red with increasing solvent polarity, indicating a substantial dipole moment of the excited state. The emission maxima of 9DPhen obtained in solvents of different polarity are reported in Table 1 together with the photophysical constants and the derived k_f and reduced k_f values according to eq 3. The

$$k_f = \frac{64\pi^4}{3h} n^3 \tilde{\nu}_{max}^3 |M|^2 \quad (3)$$

wavelength shift between isooctane and acetonitrile corresponds to an energy difference of 4600 cm^{-1} and indicates a highly polar emitting state. The absorption and emission spectra of 9DPhen were compared to those of 9PhPhen.

The positions of the absorption maxima of 9PhPhen in isooctane (λ_{max}: 334, 342, and 351 nm) resemble quite well those of 9-ethylphenanthrene,[79] and the extinction coefficient of 9PhPhen in isooctane (351 nm) has a value of 340 L mol^{-1} cm^{-1}. The emission spectrum of 9PhPhen (λ_{max}: 355, 373, and 390 nm) is also comparable with the emission of 9-ethylphenanthrene[79] and shows virtually no solvent dependence (Table 1).

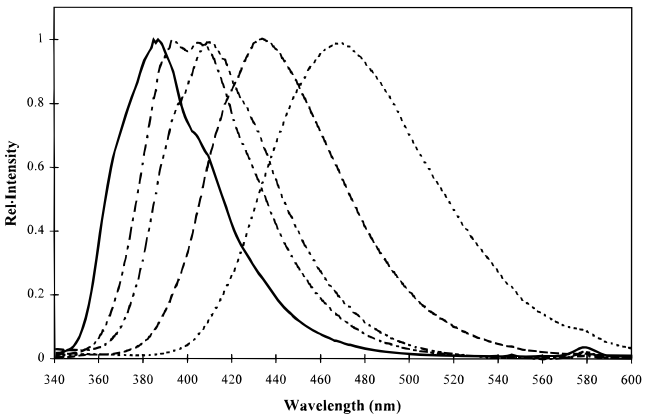

Figure 3. Fluorescence emission spectra of 9DPhen as a function of the solvent polarity at room temperature. (excitation wavelength is 295 nm): (—) isooctane, (— - —) dibutyl ether, (— - -) diethyl ether, (— —) tetrahydrofuran, and (- - -) acetonitrile.

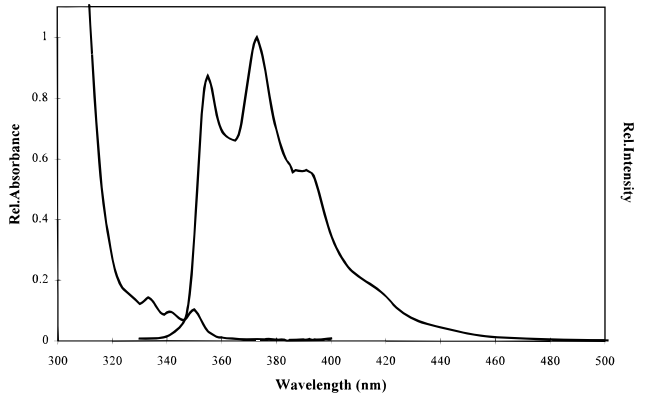

Figure 4. Absorption and emission spectra of 9PhPhen in isooctane at room temperature.

Table 1. Solvent Effects on the Spectral Position of the CT Fluorescence Maxima, Quantum Yields for Fluorescence, and Decay Parameters of 9DPhen and 9PhPhen in Solution

solvent	$\tilde{\nu}_{max}$ (cm^{-1})	Φ_f	$\langle\tau\rangle$ (ns)	$\langle k_f\rangle/10^7$ s^{-1}	$(\langle k_f\rangle/n^3\tilde{\nu}^3) \times 10^{-6}$ s^{-1} cm^3
			9DPhen		
isooctane	25 939	0.36	9.2	3.9	0.8
dibutyl ether	25 316	0.44	2.42	19.4	4.4
diisopropyl ether	24 631	0.49	2.21	22.2	5.5
diethyl ether	24 570	0.49	2.16	22.7	6.2
butyl acetate	23 474	0.62	2.73	22.7	6.5
ethyl acetate	23 255	0.65	3.6	18.1	5.6
tetrahydrofuran	23 148	0.68	2.7	20.7	6.0
acetonitrile	21 321	0.85	7	12	5.1
			9PhPhen		
isooctane	25 641[a]	0.23	41.1	0.56	0.12
acetonitrile	25 641[a]	0.39	38.4	1.02	0.25

[a] 0−0 transition.

For 9DPhen, the dipole moment of the highly polar state can be determined by the fluorescence solvatochromic shift method[80−86] (Figure 5), given that the excited state lives sufficiently long with respect to the orientational relaxation time of the solvent, smaller than 0.1 ns in every case, and assuming a point dipole situated in the center of the spherical cavity. Neglecting the dipole moment of the ground state and the

(84) Bakshiew, N. G. *Opt. Spektrosk.* **1961**, *10*, 717.
(85) Bilot, L.; Kawski, A. *Z. Naturforsch.* **1962**, *17A*, 621.
(86) Liptay, W. *Z. Naturforsch.* **1965**, *20A*, 1441.

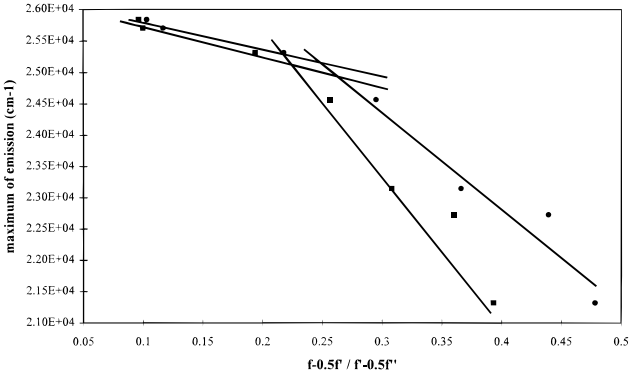

Figure 5. Lippert−Mataga plot: fluorescence emissiom maximum as a function of the solvent polarity parameter $f - 0.5f'$ (without solute polarizability) and $f - 0.5f''$ (including solute polarizability): (■) $f - 0.5f'$ and (●) $f - 0.5f''$.

polarizability (α) of the solute in the states involved in the transition, one can derive the following equations:[87,88]

$$hc\tilde{\nu}_{CT}^{max} = hc\tilde{\nu}_{CT}^{max}(0) - \frac{2\mu_e^2}{a_0^3 4\pi\epsilon_0 hc}\left(f - \frac{1}{2}f'\right) \qquad (4)$$

$$\left(f - \frac{1}{2}f'\right) = \left(\frac{\epsilon_r - 1}{2\epsilon_r + 1}\right) - \frac{1}{2}\left(\frac{n^2 - 1}{2n^2 + 1}\right) \qquad (5)$$

$\tilde{\nu}_{max}$ and $\nu_{max}(0)$ correspond, respectively, to the wavenumber of the emission maximum in a solvent with dielectric constant ϵ and refractive index n and the wavenumber of the emission maximum in the gas phase. ϵ_0, h, c, and a_0 correspond to the permitivity of vacuum (8.85×10^{-12} J^{-1} C^2 m^{-1}), the Planck constant (6.62×10^{-34} J), and the velocity of light in a vacuum (2.99×10^8 m/s). For 9DPhen we estimate an Onsager radius a_0 of the solvent cavity of 5.7×10^{-10} m by analogy with the Onsager radius calculated for the compound 1-(*N*,*N*-diethylanilino)pyrene.[52] μ_e (Cm^{-1}) is the permanent dipole of the excited state.

As can be seen in Figure 5, the experimental results do not follow the linear relationship predicted by eq 4. The change in slope is observed between the solvents dibutyl ether and diethyl ether. Assuming that μ_g equals zero, a value of 24 500 cm^{-1} is obtained for the ratio of $-2\mu_e^2/a_0^3 4hc\pi\epsilon_0$ ($\mu_e = 21.2$ D) in the region of highly polar solvents. In the region of less polar solvents, a linear relationship with a slope of 4800 cm^{-1} can be drawn from which a dipole moment of 9.3 D can be derived.

The deviation from the linear equation could be caused by the large contribution of the induced dipole moment in the excited state involved in the transition. In the former equation, the polarizability of the solute was neglected but the influence of the induced dipole moment can be taken into account by postulating the polarizability $\alpha_g \equiv \alpha_e \equiv \rho^3/3$ for respectively the ground and the excited state.[89−90]

The obtained solvent polarity parameter $f - 0.5f''$ (eq 7) leads to a new plot of $\tilde{\nu}_{max}$ as a function of the solvent polarity (Figure 5).

$$hc\tilde{\nu}_{CT}^{max} = hc\tilde{\nu}_{CT}^{max}(0) - \frac{2\mu_e^2}{4\pi\epsilon_0 hc a_0^3} f''(\epsilon_r, n) \qquad (6)$$

$$f''(\epsilon_r, n) = \frac{\left(\frac{\epsilon_r - 1}{2\epsilon_r + 1}\right)}{1 - \left(\frac{\epsilon_r - 1}{3(2\epsilon_r + 1)}\right)} - \frac{\left(\frac{n^2 - 1}{2(2n^2 + 1)}\right)}{1 - \frac{(n^2 - 1)}{3(2n^2 + 1)}} \qquad (7)$$

Taking into account this polarizability there is still a deviation from linearity (Figure 5). The nonlinear behavior, even with the correction for the polarizability, could be explained by an equilibrium between two excited states or by a continuous change in the excited-state wave function as a function of solvent (vide infra).

While the change of slopes clearly indicates some relaxation process depending on solvent polarity, the absolute values of the excited-state dipole moments should be viewed with caution. One should take into account that the solvatochromic method is rather crude in predicting absolute values of μ_{CT} as there is a certain arbitrariness in the choice of the Onsager radius value.

For 9DPhen, the determined fluorescence quantum yields strongly depend upon the solvent polarity as can be seen in Table 1. The higher the solvent polarity, the larger the quantum yield of fluorescence.

In contrast with the solvent dependence of 9DPhen, the fluorescence quantum yields of 9PhPhen are quite solvent independent. The quantum yield of 9PhPhen did amount to 0.23 in isooctane and in dibutyl ether and to a value of 0.26 in diethyl ether and tetrahydrofuran. Only in acetonitrile is a small increase of the quantum yield (0.39) observed (Table 1).

In a rigid matrix (isopentane, 77 K), the structure of the emission band of 9DPhen was very similar in shape with the emission spectra of 9DPhen in isooctane at room temperature. Also in a rigid matrix of a more polar solvent ethanol, the structure of the emission band of 9DPhen was very similar in shape to the emission spectra of 9DPhen in isooctane at room temperature.

In this rigid matrix system also a stuctureless phosphorescence was observed which differed distinctly in shape and position from the phosphorescence of 9-ethylphenanthrene and 9-phenylphenanthrene as can be seen in Figure 6.

Because of this noticeable difference in phosphorescence also nanosecond transient absorption measurements were performed for 9DPhen and 9PhPhen in diethyl ether. As can be seen in Figure 7, the difference in the transient absorption spectra of the two compounds spectra is quite obvious.

When the transient absorption spectra of 9DPhen were measured in solvents of different polarity a clear shift of the absorption bands was observed as can be seen in Table 2. In very polar solvents (acetonitrile), however, the shape of the transient absorption band is changed compared to that of the medium polar solvents, and at long delay times (50 μs), an absorption at 436 nm remains, the contribution of which increases with increasing laser energy. This suggests that the remaining absorption could be caused by photoionization.

Single Photon Timing Experiments. Using single curve analysis, the fluorescence decay of 9DPhen in isooctane, dibutyl ether, diisopropyl ether, diethyl ether, butyl acetate, ethyl acetate, tetrahydrofuran, ethanol, and acetonitrile could be analyzed as a single exponential decay and the fluorescence lifetime does not depend upon the analysis wavelength. Also by global analysis, the fluorescence decays obtained at different emission wavelengths could be analyzed as a single exponential decay ($Z_\chi^2 < 3$).

(87) Liptay, W. In *Excited States*; Lim, E. C., Ed.; Acadamic Press: New York, 1974; p 129.
(88) Baumann, W.; Nagy, Z.; Maiti, A. K.; Reis, H.; Rodriges, S. V.; Detzer, N. *Yamada Conference XXIX on Dynamics and Mechanisms of Photoinduced Electron Transfer and related Phenomena*, Osaka, Japan; Mataga, N., Okada N., Masuhara, H., Eds.; Elsevier: Amsterdam, 1992; p 211.
(89) van der Zwan, G.; Hynes, J. T. *J. Phys. Chem.* **1985**, *89*, 4181.
(90) Suppan, P. *Chem. Phys. Lett.* **1983**, *94*, 272.

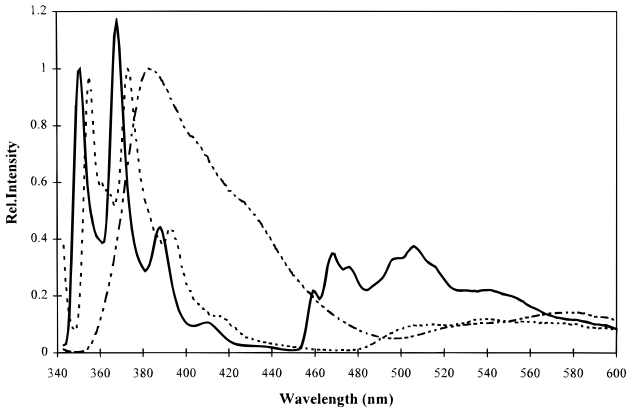

Figure 6. Emission spectra of 9DPhen (— - -), 9-ethylphenanthrene (—), and 9PhPhen (- - -) in a rigid matrix: isopentane, 77 K.

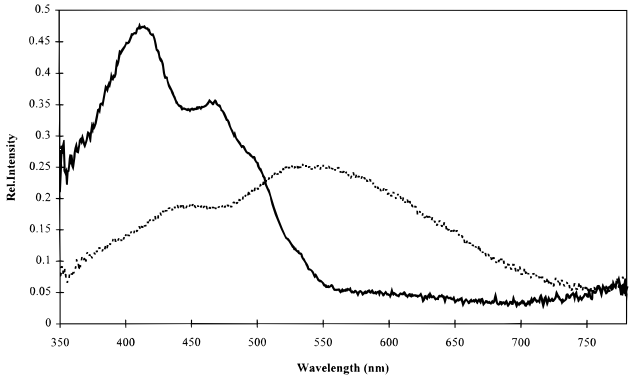

Figure 7. Subnanosecond transient absorption spectra of 9DPhen (- - -) and 9PhPhen in diethyl ether (delay time and pulse width of 100 ns).

Table 2. Spectral Shift of the Transient Absorption Bands of 9DPhen in Solvents of Different Polarity (laser energy: 27 mJ)

solvent	λ(max1) (nm)	λ(max2) (nm)	I_{max2}/I_{max1}
isooctane	530	448	1.30
diethyl ether	542	446	1.32
ethyl acetate	555	446	1.41
THF	562	441	1.13
butanol	564	440	1.04

In acetonitrile some additional experiments were performed at the blue edge of the emission spectrum, down to 380 nm. In these experiments, a time increment of 5.3 ps was used and a scatter solution as a reference. For these conditions also a single exponential decay was obtained which could be analyzed together globally with the earlier experiments.

In Table 1, the decay times of 9DPhen and 9PhPhen are reported as a function of the solvent polarity.

In analogy with the spectral similarity between 9PhPhen and 9-ethylphenanthrene, the decay time did not vary that much upon increasing the solvent polarity; in isooctane, it amounted to 57.6 and 41.1 ns for 9-ethylphenanthrene and 9PhPhen, respectively. In acetonitrile the decay times amounted to 55.2 and 38.4 ns, respectively. Judging from these experiments the first excited states of 9-ethylphenanthrene and 9PhPhen seem quite similar (Table 1).

The single exponential decay of 9DPhen in all solvents can be explained by the presence of a single excited state, the nature of which is changing as a function of the solvent polarity or by a fast equilibration between two excited-state minima with different properties. Three origins for the change with solvent polarity could be suggested:

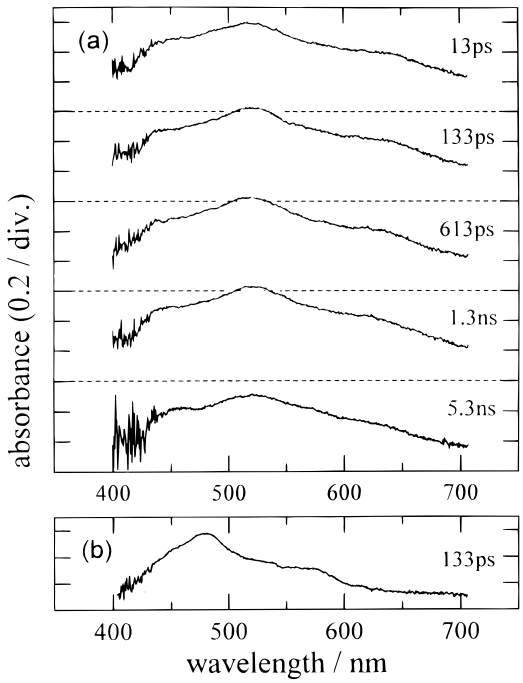

Figure 8. (a) Picosecond transient absorption spectra of 9DPhen in isooctane. (b) Transient absorption spectrum of 9PhPhen in isooctane.

(I) A quantum chemical mixing (configuration interaction) leading to mixed wave functions for a single conformation. This mixing will be strongly angle dependent. For a 90° twist, the ICT state converges to the classical TICT state.[34,54]

(II) A broadened potential minimum due to a rotational distribution of conformers in the emitting state which changes with solvent polarity. This distribution will change with solvent polarity if the excited-state potential is solvent polarity dependent.

(III) Solvent dependency of the relative population of the minumum. In the equilibrium model, the relative population of the minimum can be solvent dependent if these possess different excited state dipole moments.

Taking into account broad angular distributions, the effective $\langle k_f \rangle$ can be written more accurately as

$$\langle k_f \rangle = \int_\theta k(\theta)\, \eta\theta\, \mathrm{d}\theta \tag{8}$$

Combining the results of stationary and time-resolved measurements, the rate constant of fluorescence $\langle k_f \rangle$ and $\langle k_f \rangle / n^3 \tilde{\nu}^3$ can be obtained using eq 9 because emission in 9DPhen is supposed to occur from a charge-transfer state formed more quickly than the time resolution of the instrumental equipment.

$$\langle k_f \rangle = \frac{\Phi_f}{\langle \tau \rangle} \tag{9}$$

The high quantum yields of fluorescence and the relatively short decay times correlate with the highly allowed nature of the emissive CT state[59] and contrast with the rather forbidden emission which is associated with a TICT state.[34,54]

Picosecond Transient Absorption Measurements. The results from the picosecond transient absorption measurements of 9DPhen and 9PhPhen in the solvent isooctane are represented in Figure 8. The transient absorption spectrum of 9PhPhen is similar to that of 9-ethylphenanthrene,[91] and the shift of the maximum is about 10 nm. This suggests that the substitution effect of the phenyl group in the phenanthrene electronic

(91) Tamai, N.; Masuhara, H.; Mataga, N. *J. Phys. Chem.* **1983**, *87*, 4461.

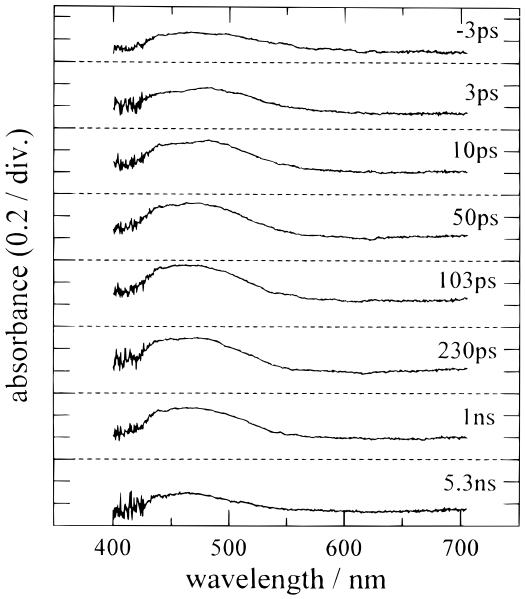

Figure 9. Picosecond transient absorption spectra of 9DPhen in acetonitrile.

structure is not large. The decay time of this species is too long to be determined accurately within the used experimental setup by the change in intensity of the absorption band.

On the other hand, 9DPhen in isooctane shows an absorption band at 520 nm, assigned to the S_1-S_n absorption of a delocalized excited state.

The bathochromic shift of 30 nm between the S_1-S_n absorption of 9-ethylphenanthrene (maximum of absorption at 490 nm in THF)[91] and the S_1-S_n absorption of 9DPhen in isooctane again is an indication for a substantial coupling between the phenanthrene and the dimethylanilino unit in the excited state, even in nonpolar solvents such as isooctane.

The decay time of 9DPhen deduced from these measurements (10 ns) is in good agreement with the the value obtained in the single photon timing experiments (9.1 ns).

In the polar solvent acetonitrile, the charge-transfer absorption band of 9DPhen is situated at 460 nm, which could be a sum of the cation of the DMA group and the anion of the phenanthrene group.[92,93] This suggests that a polar electronic structure is formed. The value of the decay time (5 ns) is in good agreement with the value obtained from the analysis of the fluorescence decay (7 ns), confirming that there was no photoionization during these experiments.

If the transient absorption spectra of 9DPhen in acetonitrile are investigated in more detail, a fast component of a few picoseconds is distinguished, which on the basis of the time resolution in SPT can be estimated to be less than 15 ps. Also if the normalized difference spectra of 9DPhen in acetonitrile are obtained after 3 and 100 ps delay times, this difference spectrum is quite similar to the spectrum of 9DPhen in isooctane.

Thus, in acetonitrile, the spectrum even at an early stage (first few picoseconds) contains the contribution of the less polar electronic structure as observed in isooctane and then changes to the more polar species.

Quantum Chemical Calculations on 9DPhen. Figure 11 shows the ground-state twist potential of 9DPhen (regarding the dihedral angle of the X-ray structure $C_{14-13-15-16}$). In agreement with the X-ray structure where a value of 64.2° was measured, the most probable twist angle φ is 62°, with a small barrier to rotation for $\varphi = 90°$ (0.3 kcal/mol or 0.013 eV) and

(92) Land, E. J.; Porter, G. *Trans. Faraday Soc.* **1963**, *59*, 2027.
(93) Shida, T.; Iwata, S. *J. Am. Chem. Soc.* **1973**, *95*, 3473.

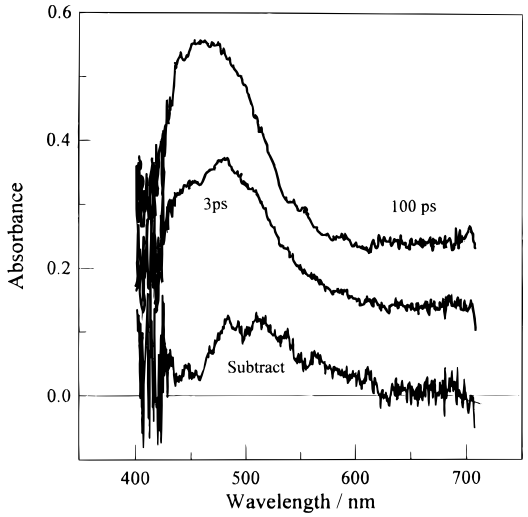

Figure 10. Normalized transient absorption spectra of 9DPhen in acetonitrile at 3 ps after excitation and at 100 ps after excitation and a difference spectrum (thick line) obtained by subtracting the spectrum 100 ps after excitation from the spectrum 3 ps after excitation.

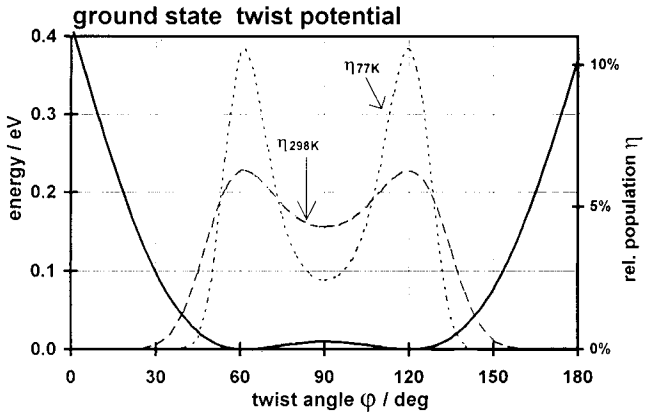

Figure 11. S_0 gas phase twist potential of 9DPhen using the AM1 method and full geometrical optimization at each twist angle. The population distribution according to Boltzmann is also given for two different temperatures.

a large one for planarity (20 kcal/mol or 0.87 eV). The accessible angular range is thus 30−150° at room temperature, with a sizable population at 90° (see Figure 11). For angles deviating from 90°, the molecule relieves additional sterical strain mainly by the following two geometrical deformations: (1) bending of the whole molecule with respect to the linking bond and, (2) loss of planarity of the phenanthrene moiety to a boatlike structure. These effects are already clearly visible at the minimum-energy geometry ($\varphi = 62°$) and get stronger for more planar geometries. They have an evident influence on the excited-state properties and lead to a larger coupling between the relevant excited states, which is discussed below (see Table 3 with a comparison of optimized and idealized geometries).

The challenging question for the quantum chemical calculations is to give some information on the nature of the lowest excited singlet state which is observed experimentally connected with an allowed and solvent polarity dependent emissive transition. Figure 12 depicts the relevant molecular orbitals (MO's) of 9DPhen involved in the low-energy transitions at 90° and at the equilibrium twist angle between the electron donor unit dimethylanilino (D) and the acceptor unit phenanthryl (A). It can be seen that for 90° the orbitals are localized on the subchromophores, and consequently, the transitions on one subunit can be assigned to local transitions of phenanthrene (A) and dimethylaniline (D). The local singlet transition of lowest

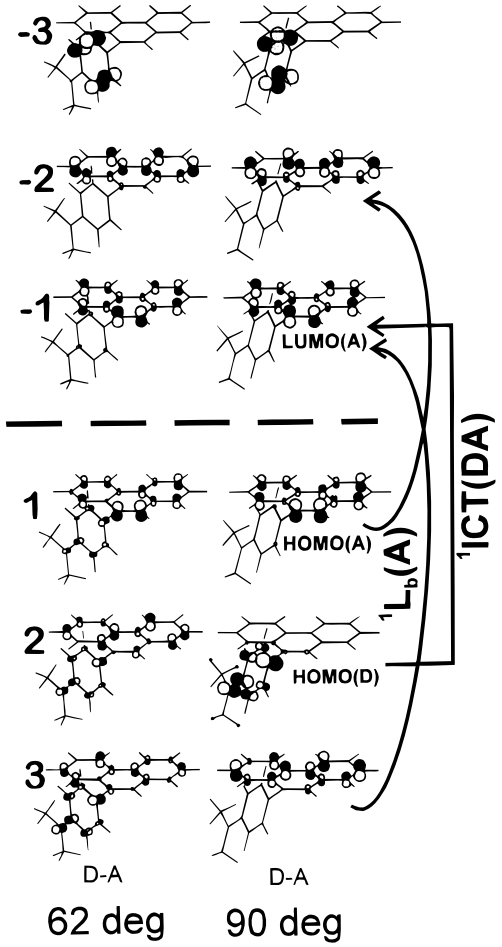

Figure 12. Molecular orbitals (MO's) of 9DPhen at perpendicular and equilibrium geometries.

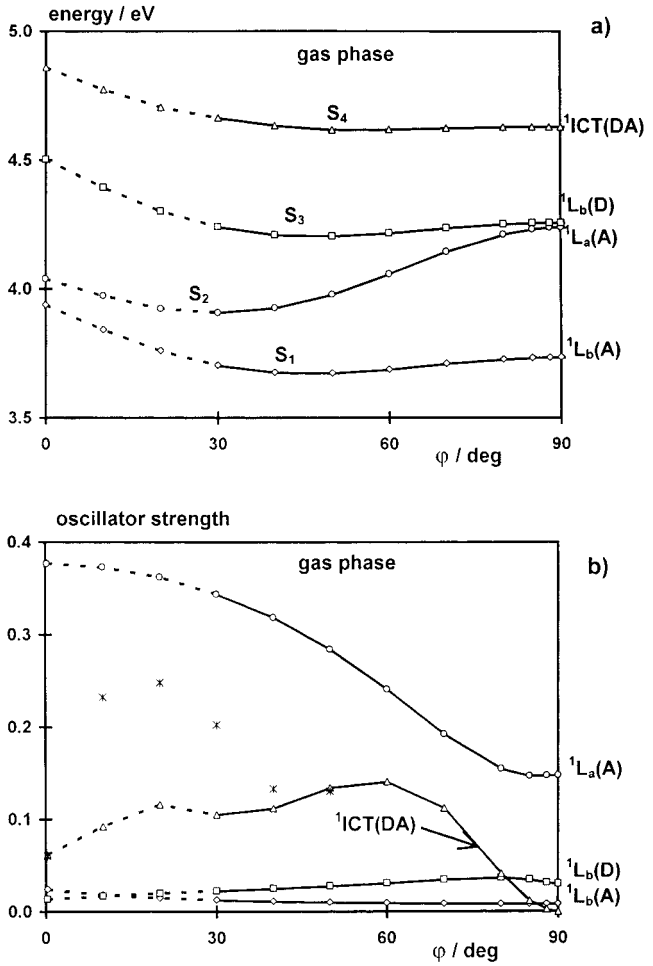

Figure 13. State energies S_1-S_4 in the gas phase (a) and the corresponding oscillator strengths (b) calculated with CNDO-S parametrization. The energies calculated using the CNDUV parametrization are similar with a maximum deviation of about 0.1 eV. The broken lines indicate the angular range that is not populated in S_0. The crosses indicate the oscillator strengths for S_4 calculated with idealized geometries.

energy is the ^1L_b(A) consisting of the one-electron transitions $1 \rightarrow -2$ and $3 \rightarrow -1$.The second local singlet transition is the ^1L_a(A) connected with $1 \rightarrow -1$ and $3 \rightarrow -2$ configurations. Transitions between the subunits are connected with a full intramolecular charge transfer (^{1}ICT (DA)), and the one of the lowest energy consists of the $2 \rightarrow -1$ or HOMO(D) $\rightarrow$ LUMO-(A) configuration. For deviations from 90°, the transitions are linked with the same configurations but the orbitals become delocalized over the subunits, especially the occupied MO's 1,2 and 3 (Figure 12). As a result all of the transitions get delocalized character and mix in some contributions of the configuration $2 \rightarrow -1$. Nevertheless, they can be regarded as keeping their substantial (spectroscopic) properties over the whole angular range and their directions and they can be correlated with the "pure" ^1L_a, ^1L_b, etc., states of D and A at 90°.

We want to express this by calling these states ^1L_a-type, ^1L_b-type, etc., for angles deviating from 90°. Due to the orbital and CI mixing, S_1-S_3 increase their dipole moments from 90° to 62°, and that of ICT (S_4) decreases, so that the dipole moments of the four lowest singlet states become rather similar at 62° (see below Figure 14a). The transition moments of the ^1L_b states (S_1 and S_3) remain quite low, and the strongest angular changes for *f* are found for S_4 (ICT) (Figure 13b).

Figure 13a summarizes the energetic angular dependence of the lowest singlet excited states in the gas phase as derived from adding the excited-state energy difference, calculated within CNDO/S, to the ground-state energy and using the appropriate optimized geometry for every twist angle. Most of the excited states are energetically flat in the region 30°−150°, similar to the ground state, with the exception of S_2 (^1L_a(A) at 90°), which is stabilized for planar conformations around 30°. There is a common tendency for shifting the energetic minima to values smaller than 60°.

The oscillator strengths (Figure 13b) indicate forbidden character for the ^1L_b states at all twist angles and for the charge-transfer state ^{1}ICT(DA) at the perpendicular geometry. For deviations from 90°, the ^{1}ICT(DA) state becomes allowed through a better overlap of the MO's involved. Similar to perpendicular geometry's, below 60°, the above-mentioned geometric deformations also disturb the overlap of the MO's concerned and therefore lead to a decrease of the oscillator strength. In contrast to the optimized geometry, the oscillator strength for the idealized geometry (with subunit structures without deformations) increases up to an angle of 20°. This indicates the necessity of a good orbital overlap for the MO's involved in ICT to obtain high oscillator strengths of the $S_0 \rightarrow S_4$ transition. Moreover geometric deformations also have a considerable influence on the mixing of the states through configuration interaction (CI). For example, the contribution of the HOMO(D) $\rightarrow$ LUMO(A) configuration to the ICT transition S_4 changes from about 53% for the idealized to about 27% for the optimized geometry at an equilibrium twist angle accompanied by an increase of this contribution to S_1 (^1L_b(A)) from 19% to 23% (see Table 3).

Table 3. Contribution of the HOMO(D) → LUMO(A) Configuration (%) to the First Four Excited Singlet States for the Perpendicular and Equilibrium Geometry[a]

		$\varphi = 90°$			$\varphi = 62°$		
state	nature	CNDUV ideal	CNDUV opt	CNDO-S opt	CNDUV ideal	CNDUV opt	CNDO-S opt
S_1	^1L_b(A)	0	0	0.001	19.3	23	11.1
S_2	^1L_a(A)	0	0.01	0.02	2.1	2.4	2.6
S_3	^1L_b(D)	0.28	0.4	0.4	0.07	0.03	0.01
S_4	^{1}ICT(DA)	88.4	85.8	84.1	52.7	26.8	37.9

[a] Idealized and optimized geometries as well as two different parametrizations are compared.

A complete CI expansion of the wave functions for the lowest four states is given in the following equations.

CI expansion for S_1 to S_4 (contributions ≥ 0.1) (from CNDO-S/opt. calculation):

90°

$$S_1 \quad (^1L_b(A)) = -0.003\chi(2-1) - 0.69\chi(1-2) - 0.58\chi(3-1) + 0.31\chi(1-1) - 0.19\chi(3-2) \quad (10)$$

$$S_2 \quad (^1L_a(A)) = +0.013\chi(2-1) - 0.84\chi(1-1) + 0.37\chi(3-2) - 0.30\chi(1-2) - 0.20\chi(3-1) \quad (11)$$

$$S_3 \quad (^1L_b(D)) = +0.064\chi(2-1) + 0.87\chi(2-3) \quad (12)$$

$$S_4 \quad (\mathrm{ICT}) = +0.92\chi(2-1) + 0.23\chi(2-7) + 0.22\chi(2-2) \quad (13)$$

62°

$$S_1 \quad (^1L_b(A)\text{-type}) = +0.33\chi(2-1) + 0.64\chi(1-2) + 0.47\chi(3-1) - 0.34\chi(2-2) + 0.27\chi(1-1) \quad (14)$$

$$S_2 \quad (^1L_a(A)\text{-type}) = +0.16\chi(2-1) - 0.87\chi(1-1) + 0.29\chi(1-2) + 0.21\chi(3-2) + 0.16\chi(2-2) \quad (15)$$

$$S_3 \quad (^1L_b(D)\text{-type}) = -0.01\chi(2-1) + 0.66\chi(1-3) + 0.41\chi(2-3) - 0.37\chi(3-3) + 0.14\chi(1-1) \quad (16)$$

$$S_4 \quad (\mathrm{ICT}) = -0.62\chi(2-1) - 0.25\chi(3-2) - 0.24\chi(3-4) + 0.24\chi(1-5) + 0.23\chi(1-2) + 0.23\chi(1-6) + 0.21\chi(2-5) + 0.21\chi(3-5) - 0.16\chi(2-6) + 0.16\chi(3-1) - 0.10\chi(2-2) - 0.10\chi(2-4) \quad (17)$$

In these equations, the ICT configuration ($\chi(2-1)$) has been included in all cases as the first member in the expansion. Note that it does not contribute to S_1-S_3 at 90° but constitutes nearly purely the S_4 state whereas it contributes to most states to a nonnegligible extent at 62°. A very strong mixing between a large number of configurations is obvious at 62°.

A simplified discussion is possible by considering the percent contribution for the various states for $\chi(2-1)$, the HOMO(D) → LUMO (A) configuration, which is contained in Table 3.

The comparison of the contribution of the HOMO(D) → LUMO(A) configuration to the various excited states (Table 3) reveals that, at 90°, S_4 is represented by this configuration alone—pure ICT corresponding to the classical TICT state,[34,54] whereas for the equilibrium angle of 62°, it is distributed over several states which can mix with the ^{1}ICT(DA) state S_4. Moreover from Table 3 it follows that at 62° there is less significant mixing of the HOMO(D) → LUMO(A) configuration

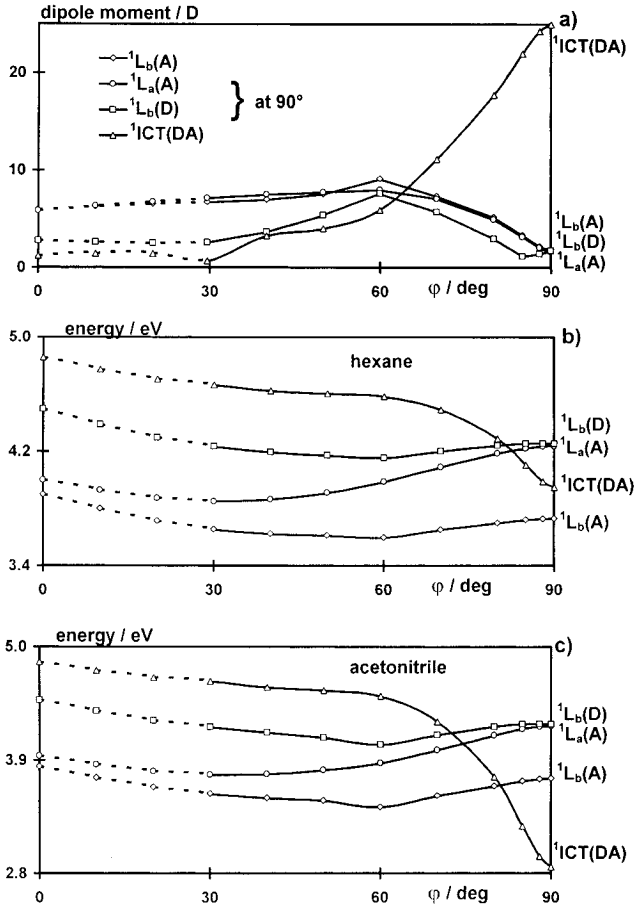

Figure 14. Dipole moments of the various excited states as a function of twist angle φ (a) and the derived solvation corrected excited state energies in *n*-hexane (b) and acetonitrile (c).

which constitutes a large part of the ^{1}ICT (DA) state S_4 with the ^1L_a(A)-type (S_2) or the ^1L_b(D)-type (S_3) states than with the ^1L_b(A)-type (S_1) and furthermore with the $1B_b$(A)-type (S_6) states, the transition moments of which are polarized in the short axis of the phenanthrene unit and thus are polarized approximately in the same direction ($\alpha_{Lb/ICT} = 30°$) as the ICT transition represented by the HOMO(D) → LUMO(A) configuration. On the other hand the transition moments of the ^1L_a(A), ^1B_a(A), and ^1L_b(D) states are close to perpendicular to that of ^{1}ICT(DA) ($\alpha_{La/ICT} = 60°$). Hence, although there is no symmetry in the molecule, in the case of the gas phase, there is enhancement of CI mixing between the ^{1}ICT(DA) and ^1L_b(A) states because of their roughly parallel transition moments.

To get an idea how solvation affects the various excited states, dipole moments were calculated and the excited-state energies derived for different solvents by adding the solvation energy (eq 2) to the gas phase energies. The results, presented in Figure 14a, show that the excited-state dipole moments are medium sized (<10 D) and tend to minimize for the perpendicular conformations, with the exception of the S_4 state (pure ^{1}ICT-(DA) at 90°), which exhibits the opposite behavior. For angles φ deviating strongly from 90°, this state is of low dipole moment due to a loss of HOMO(D) → LUMO(A) contribution (Table 3) and due to the enhanced delocalization of the MO's involved (Figure 12). The large dipole moments for the more twisted conformations lead to a strong energetic lowering for the ICT state (Figure 14 b,c). As a consequence, in highly polar solvents, a nearly pure ICT state with perpendicular conformation becomes the lowest excited state, whereas in weakly and medium polar solvents, the energetic closeness should result in

an enhanced mixing of the ^{1}ICT(DA) with the ^1L_b(A) and furthermore with the ^1L_a(A) state.

The relative mixing strength with these two LE states is expected to be strongly polarity dependent. Such a behavior is indicated by the curved nature of the solvatochromic plot (Figure 5) which yields a calculated dipole moments of 18 D in medium and highly polar and 9 D in weakly polar solvents, respectively. The latter value is in good agreement with the calculated dipole moment of about 8 D of the lowest excited singlet state at equilibrium geometry which is of ^1L_b(A) nature. But the fact that the oscillator strength of this state is strongly underestimated indicates that the allowed ICT character is underestimated by the calculation. It has to be kept in mind that the quantum chemical calculations yielding the *f* values, are done for the gas phase, not for the solvated phase which are the conditions of the experiments. To treat the problem properly, a program which includes the solvation energy in the Hamiltonian should be used. Two sources of mixing which possibly are considered insufficiently by the gas phase calculations may serve to describe the experimental observations: (a) solvent-dependent configuration interaction (CI) between configurations with LE and ICT character and (b) mixing of donor and acceptor MO's yielding delocalized orbitals.

As can be seen from Figure 12 the second occupied MO HOMO(D) (MO 2 at 90°) strongly interacts with the neighboring MO's because they are very close in energy. The MO mixing of the HOMO(D) to MO's 1 and 3 involved in the ^1L_b(A) as well as the ^1L_a(A) transition (Figure 12) gets enhanced for more planar geometries diluting the localized character of S_1 and introducing ICT without necessitating CI.

In an attempt to evaluate this orbital coupling, we adjusted the parametrizations such that the HOMO(D) became energetically situated above the HOMO(A) at 90° (compare Figure 12 where HOMO(D) is situated energetically below HOMO(A)). The resulting mixed MO's at 62° are then qualitatively different from those in Figure 12, namely orbital 3 loses its donor contribution whereas MO's 1 and 2 both contain a large weight of HOMO(D). Consequently, the $1 \rightarrow -1$ transition, which contributes to the ^1L_a(A) state, gets a much stronger ICT character leading to a ^1L_a(A)/ICT state that is energetically close to S_1 (^1L_b(A)) and connected with an increased dipole moment and oscillator strength. It cannot be excluded that this change of orbital coupling, which we simulated here by a change of parameters, may be induced also by differently polar solvents. Already medium-polar solvents may then be expected to lead to a level crossing of S_1 (^1L_b(A)) and S_2 (^1L_a(A)/ICT).

The principle of MO mixing can also explain the ^1L_b character of S_1 in 9PhPhen. Here, the HOMO of the phenyl unit is situated considerably below the two highest occupied MO's of phenanthrene. Thus the MO interaction is only very weak and the lowest transition is of rather pure ^1L_b(A) nature at all twist angles. The increased influence of MO mixing in 9DPhen gets obvious by the comparison of the calculated oscillator strengths for the ^1L_b states. The relative weights for the gas phase are $f_{9DPhen}:f_{9PhPhen}:f_{Phen} = 6.6:3.3:1$.

Conclusions

For 9DPhen, the spectral shift of the second absorption band as a function of the solvent polarity indicates the interaction between the dimethylanilino and the phenanthrene unit in the ground state. This could correspond to the mixing (through orbital overlap and CI) of the ^1L_a and ^1L_b states with the CT state related to the formation of delocalized orbitals.

The bathochromic shift of the emission spectra and the resulting dipole moment value in polar solvents are clear evidence that the excited state emitting in high-polarity solvents has a pronounced charge-transfer character.

The nonlinear dependence of the maximum of the emission as a function of the solvent polarity and the solvent dependences of k_f and $k_f/\tilde{\nu}^3n^3$, are an indication that emission in all solvents occurs from a fluorescent CT state with a solvent-dependent electronic structure. In polar media the spectrum differs markedly between the frozen and liquid solvents, which can be an indication of a change in the conformational distribution after excitation or can be explained by solvent relaxation alone.

According to the mixing of the wave functions on the one hand and the conformational distribution on the other hand which both contribute to the change of the electronic structure with increasing solvent polarity, k_f is first strongly increasing, due to the narrowing of the energy difference of ICT and S_1 or S_2, and then decreasing slightly again in highly polar solvents, explainable by a larger contribution of more twisted conformations. For 9PhPhen, with no low-lying ICT state, k_f is not polarity sensitive.

The highly allowed CT emission properties, even in acetonitrile, however, lead to the questioning of a classical TICT model assuming a relaxed state of perpendicular geometry. On the other hand, a simple geometry relaxation toward planarity in polar solvents cannot totally explain the high dipole moments and the observed variation of k_f.

A more realistic model would involve rather broad angular distributions with significant population of nonperpendicular conformations possessing increased transition moments even if the energetic minimum would be located at 90°.

The calculation indicates strong angular changes of f mainly in the neighborhood of 90°, i.e. for the more twisted conformations.

At low twist angles there is no solvent-induced state mixing possible.

The single exponential decay obtained by SPT experiments and the rapid decay of the delocalized less polar state absorption in acetonitrile suggests a solvent-assisted relaxation on a time scale of a few picoseconds to a single polar fluorescent charge-transfer state or to an ensemble of excited-state species with a different angular distribution on a time scale that is faster than the resolution of the experimental setup of SPT.

From the quantum chemical calculations and the comparison with the experiments, the following conclusions can be drawn: In the ground state, there is a significant population of perpendicular twist angles and conformations below 20° are unavailable. According to the gas phase calculations, the state which is strongly angle and polarity dependent is the state which is correlated to S_4, the ^{1}ICT(DA) state for twisted conformations. Its involvement is confirmed experimentally by the solvatochromic experiments.

The first excited singlet state S_1 is calculated as a ^1L_b state of phenanthrene but gains ICT character by two mixing phenomena, i.e. orbital mixing and configuration interaction. The mixed ^1L_a(A)/ICT character of the calculated S_2 state strongly depends on the parametrization, and thus, polar solvents may lead to a solvent-induced level crossing of S_1 and S_2. This mixing model can also explain the curved solvatochromic plot and the variation of k_f with solvent polarity. In weakly polar solvents ^{1}ICT(DA) mixes into ^1L_b(A) and/or ^1L_a(A), leading to the enhanced k_f compared to that of phenanthrene ^1L_b emission.

In polar solvents, CI mixing becomes stronger because of a sizably reduced energy gap between the first two locally excited (LE) singlet states and ^{1}ICT(DA), and furthermore, a solvent-induced level reversal of S_1 and S_2 may take place.

(94) Onkelinx, A.; De Schryver, F. C.; Iwai, K. To be published.

In the related molecule 9PhPhen, k_f is not solvent dependent and S_1 retains its forbidden $^1L_b(A)$ character as there is no low-lying ICT state.

The angular relaxation in the excited state most probably occurs toward planarity in low-polarity surroundings because, in this case, 9DPhen possesses no low-lying ICT similar to that of 9PhPhen. However, in medium polar solvents, the ICT of 9DPhen becomes low lying, leading to an enforced coupling between the LE states with the ICT(DA). As a consequence, potentials with polarity-dependent minima may arise.

In highly polar solvents relaxation is, as suggested by preliminary experiments on sterically hindered derivatives, restricted to the neighborhood of 90° twist,[94] which indeed indicates a strong reduction of k_f consistent with the calculated low oscillator strengths for the perpendicular conformations.

If, based on the quantum mechanical calculations, a population distribution of different torsional angles is assumed which is changed with the polarity of the solvent, the observed emission can be understood as being due to more than one species but in fast equilibrium and k_f is a weighted average of the values of k_f for the different species. In this case it is more accurate to speak of an average k_f value $\langle k_f \rangle = \Phi_f/\langle \tau \rangle$.

Acknowledgment. A.O. thanks the I.W.T. for financial support. M.V.D.A. is an "Onderzoeksleider" of the Belgian "Fonds voor Kollektief Fundamenteel Onderzoek". The continuing support of the Belgian "Fonds voor Kollektief Fundamenteel Onderzoek" and the DWTC through IUAP-II-16 and UIAP-II-040 is gratefully acknowledged. We thank Prof. Th. Bally (Fribourg) for the program MOPLOT.

JA953697A